JOURNAL OF AGRICULTURAL AND FOOD CHEMISTRY
ARTICLE

J. Agric. Food Chem. 2009, 57, 10313–10322 10313
DOI:10.1021/jf902586n

Interactions between Wine Volatile Compounds and Grape and Wine Matrix Components Influence Aroma Compound Headspace Partitioning

Anthony L. Robinson,[†] Susan E. Ebeler,*[,§] Hildegarde Heymann,[§] Paul K. Boss,[#] Peter S. Solomon,[⊥] and Robert D. Trengove[†]

[†]Separation Science Laboratory, Murdoch University, Murdoch, Western Australia 6150, Australia, [§]Department of Viticulture and Enology, University of California, Davis, California 95616, [#]CSIRO Plant Industry and Food Futures Flagship, P.O. Box 350, Glen Osmond, South Australia 5064, Australia, and [⊥]Plant Cell Biology, Research School of Biology, The Australian National University, Canberra, Australian Capital Territory 0200, Australia

A full-factorial design was used to assess the matrix effects of ethanol, glucose, glycerol, catechin, and proline on the volatile partitioning of 20 volatile compounds considered to play a role in wine aroma. Analysis of variance showed that the two-way interactions of ethanol and glucose, ethanol and glycerol, and glycerol and catechin significantly influenced headspace partitioning of volatiles. Experiments were conducted to observe the effect of varied ethanol and glucose concentrations on headspace partitioning of a constant concentration of volatiles. Analysis of variance and linear regression analysis showed that the presence of glucose increased the concentration of volatiles in the headspace, whereas increasing ethanol concentration was negatively correlated with headspace partitioning of volatiles. A subsequent study assessed the effect of diluting white and red wines with water and ethanol. It was again observed that increased ethanol concentration significantly reduced the relative abundance of volatile compounds in the sample headspace. This study investigates some of the complex matrix interactions of the major components of grape and wine that influence volatile compound headspace partitioning. The magnitude of each matrix−volatile interaction was ethanol > glucose > glycerol > catechin, whereas proline showed no apparent interaction. The results clearly identify that increasing ethanol concentrations significantly reduce the headspace concentration of volatile aroma compounds, which may contribute to explaining recent sensory research observations that indicate ethanol can suppress the fruit aroma attributes in wine.

KEYWORDS: GC-MS; solid-phase microextraction; ethanol; glucose; glycerol; catechin; matrix interaction; volatile partitioning; aroma

INTRODUCTION

Understanding the factors that influence the release of volatiles from the wine matrix is of major importance to understanding wine aroma perception (*1*). The sample matrix can be defined as the components of a sample other than the component of interest (*2*). In the assessment of volatiles in grape juice and wine, the matrix predominantly consists of the nonvolatile components including sugars, ethanol (in wine), organic acids, amino acids, phenolic compounds, proteins, and inorganic ions in water.

Headspace solid-phase microextraction (HS-SPME) has been increasingly utilized in volatile flavor analysis since it was introduced as a technique by Janusz Pawliszyn in the 1990s (*3*−*7*). The primary advantage of this technique is that it combines analyte extraction and preconcentration in a single step. The combined effect of the sample matrix components on the measurement of volatile compounds must be understood to accurately characterize the composition of grape and wine volatiles.

In recent years a number of studies have optimized the HS-SPME sampling conditions required to sample grape and wine matrices for target analytes. These analytes include ethyl esters, acetates, acids, and alcohols (*8*), monoterpenes and norisoprenoids (*9*), methoxypyrazines (*10*), thiols, sulfides, and disulfides (*11*, *12*), and furfural derivatives, phenolic aldehydes, volatile phenols, and oak lactones (*13*). However, the application of this technique for quantitative analysis has necessitated greater understanding of the matrix influences on volatile compound partitioning into the headspace and subsequent sorption by the SPME fiber.

Most methods described within the literature explore the parameters of fiber type, incubation time, temperature, salting concentration, and degree of agitation as part of their development (*9*, *13*−*18*). Commonly, an internal standard is utilized allowing the researcher to compensate for the matrix effects of the solution, presuming that volatile compounds partition into the headspace in equivalent ratios.

*Corresponding author [telephone (530) 752-0696; fax (530) 752-0382; e-mail seebeler@ucdavis.edu].

Published on Web 10/21/2009

Research by Câmara et al. (*9*) and Hartmann et al. (*10*) using model aqueous solutions showed that increased ethanol concentrations reduce the amount of analyte absorbed onto SPME fibres. Conner et al. (*19*) reported that below 17% (v/v), concentrations typical of table wines, ethanol in water forms a monodispersed aqueous solution, which has limited capacity to retain hydrophobic volatile compounds in solution. This observation is supported by Athès et al. (*20*) and Conner et al. (*21*), who demonstrated that increasing ethanol concentration in model aqueous solutions reduced the headspace partition coefficient of some volatile alcohols, aldehydes, and esters.

This matrix influence on headspace partitioning of volatiles is expected to have a major impact on the sensory perception of the wine. Recent sensory research has shown that ethanol exerts a suppression effect on "fruity" notes in model wine solutions (*22*−*24*). This has been considered to be due to the increased solubility of the volatiles in the solution by ethanol (*24*) and, in part, due to the inhibition of the volatile compound odor activity by ethanol (*22*). Understanding this effect is particularly important when one is trying to discern which volatile compounds are considered to be contributing to the perception of wine aroma.

Previously, wine sensory research has focused on correlating descriptive sensory and quantitative analytical data to successfully identify odor compounds that contribute to the overall aroma perception of wine (*25*−*30*). The use of sensory evaluation to elucidate the impact of complex aroma compound interactions including masking and enhancing effects is likely to improve our understanding of the perceived aroma of wine (*31*). For example, β-damascenone is recognized universally as a potent wine aroma compound (*32*,*33*) due to its low aroma threshold of 2 ng L^{-1} (*34*) in water or 50 ng L^{-1} (*25*) in 10% aqueous ethanol. A range of threshold values for model wines have been reported and are well documented in a recent publication by Pineau et al. (*33*). It has been suggested that at relatively low concentrations, β-damascenone has the ability to mask the "herbaceous" aroma associated with 2-isobutyl-3-methoxypyrazine (*33*) and the ability to enhance the "berry fruit" aromas in red wines (*23*, *33*).

It has previously been suggested that changes in threshold values may arise from changes in the headspace partition coefficient of a compound as a result of either a change in solubility or an interaction with other solute components (*19*). This is consistent with the different odor thresholds reported in water, aqueous ethanol model solutions, and model white and red wines (*33*).

The objective of this study was to observe the influence that major grape and wine matrix components have on the partitioning of volatile compounds into the headspace of model solutions and to study the effect of varied ethanol concentrations in commercially available wines. An additional benefit of this study was that we would be able to observe the impact that the matrix has on the headspace partitioning of impact odor compounds such as β-damascenone and 2-isobutyl-3-methoxypyrazine.

EXPERIMENTAL PROCEDURES

Analytical Reagents and Supplies. Polydimethylsiloxane (PDMS) SPME fibers, 100 μm 23 ga, were purchased from Supelco (Bellefonte, PA). Prior to initial use, all new fibers were conditioned for 30 min at 250 °C as per the manufacturer's recommendations. Amber glass, screw threaded, 20 mL headspace vials with magnetic screw caps and white PTFE/blue silicone (thickness = 1.3 mm) septa were purchased from Alltech Corp. (Deerfield, IL). The following chemicals were purchased: ethanol 200 proof (Gold Shield, Hayward, CA); D-glucose anhydrous (Fisher Scientific, Fair Lawn, NJ); (+)-catechin, 98%, L-proline, and potassium hydrogen tartrate, 99% (Sigma, St. Louis, MO); and glycerol (EMD Chemicals Inc., Gibbstown, NJ). Milli-Q water (Millipore, Bedford, MA) was purified to a level of 18 MΩ.

Characterization of matrix interactions was performed using artificial matrices spiked with a stock mixture of volatile chemical standards prepared in 200 proof ethanol. These chemical standards and their respective concentrations after dilution in the artificial matrix solutions are listed in **Table 1** and will be commonly referred to as the volatile standard mix. The artificial matrices are described below. A C8−C20 alkane standard mixture, used for determination of Kovats retention indices (RI), was obtained from Fluka (Sigma-Aldrich, St. Louis, MO). Studies with commercially available wines were conducted using a 2006 vintage Australian Chardonnay (14.0% ethanol vol vol^{-1}) and a 2005 vintage Australian Cabernet Sauvignon (14.0% ethanol vol vol^{-1}).

Instrumentation. All experimentation was conducted using a Gerstel MPS2 autosampler with agitator (Baltimore, MD) coupled to an Agilent 6890N gas chromatograph with an Agilent 5975 inert mass selective detector (Little Falls, DE). The GC oven was equipped with a 30 m DB-WAX capillary column with an inner diameter of 0.25 mm and a film thickness of 0.25 μm (J&W Scientific, Folsom, CA) with a 0.75 mm inner diameter SPME inlet liner (Supelco, Bellefonte, PA).

Chromatographic Conditions. The injector was held at 250 °C in the splitless mode with a purge-off time of 1 min, a 50 mL min^{-1} split vent flow at 1 min, and a 20 mL min^{-1} gas saver flow at 5 min. Ultrahigh-purity (UHP) helium (Praxair, Danbury, CT) was used as the carrier gas at a constant flow rate of 1.2 mL min^{-1}. The temperature program was 40 °C for 1 min, 5 °C min^{-1} to 185 °C, then 40 °C min^{-1} to 240 °C, held for 3.62 min, with a total run time of 35 min. The transfer line and ion source were maintained at 240 and 230 °C, respectively. The detector collected masses between 40 and 240 amu with a scan rate of 6.61 scans s^{-1}.

Optimization of SPME Extraction Time. Samples were incubated at 30 °C with agitation at 500 rpm for 5 min and allowed to rest for an additional 5 min prior to extraction. The headspace was sampled for 1, 2, 5, 10, 15, 20, 25, 30, 45, and 60 min periods with the vial at ambient temperature (25 ± 2 °C). The fiber was desorbed in the inlet at 250 °C for 1 min. The fiber was then reconditioned in the inlet for a further 4 min to prevent analyte carry-over between samples. The relative responses of compounds were assessed in relation to the specific optimization parameter through hierarchical cluster analysis using a minimal variance algorithm (*35*). Compound cluster membership (compounds that responded similarly to the optimization parameters) was then analyzed using a one-way analysis of variance (ANOVA) to determine whether compound clusters responded differently to the specified optimization parameter (**Table 1**). Cluster means were then plotted against the extraction time.

GC-MS Data Analysis Software. GC-MS interrogation and spectral deconvolution were conducted using AMDIS ver. 2.65 (Build 116.66) [National Institute of Standards and Technology (NIST), Gaithersburg, MD] (*36*) using a component width of 32 scans, two adjacent peak subtractions, and high sensitivity, resolution, and shape requirements. Compound mass spectral data were compared against the NIST 2005 Mass Spectral Library, and calculated retention indices were compared to published retention indices (*37*−*43*) for identity confirmation. Peak area integration of unique masses was conducted using MSD Chemstation (G1701-90057, Agilent).

Statistical Analysis Software. Statistical analysis was conducted using JMP version 7.0.1 (SAS Institute Inc., Cary, NC). Figures and tables were generated using Microsoft Office Excel 2007 (Microsoft Corp., Redmond, WA).

Experimental Design. Potassium hydrogen tartrate was added to all model solutions at a rate of 6 g L^{-1}, creating a super-saturated solution at 25 °C (*44*). The addition of potassium hydrogen tartrate provided buffering capacity to the solution, and for all practical purposes provides a pH of 3.57 ± 0.02 (*45*). Each solution was spiked with the volatile standard mix at 10 μL mL^{-1} to give a final concentration, listed in **Table 1**, of each compound. All samples were analyzed in triplicate with the exception of the study assessing the interaction effects of major grape and wine matrix components, for which samples were analyzed in duplicate. Sample sequence order was randomized within replicate blocks using a random number generator (http://www.random.org) in all experiments.

Interaction Effects of Major Grape and Wine Matrix Components. A full-factorial design was used to assess the influence of ethanol

Table 1. Volatile Chemical Standards Used for the Characterization of Wine Matrix Effects

compound	CAS Registry No.	concn (μg L^{-1})	manufacturer[a]	purity (%)	MW	Log D[b]	unique ion[d]	cluster[c]	RT (min)	RI calcd[e]	RI lit.[f]	ref (lit.)
ethyl 2-methylbutyrate	7452-79-1	2068	Aldrich	99	130.18	2.12	102	1	4.417	1048	1056	(*40*)
ethyl 3-methylbutyrate	108-64-5	2184	Aldrich	98	130.18	2.12	88	1	4.689	1064	1068	(*39*)
isoamyl acetate	123-92-2	2108	Aldrich	98	130.18	2.12	43	1	5.763	1120	1125	(*39*)
limonene	5989-27-5	21	Sigma-Aldrich	97	136.23	4.45	93	3	7.386	1193	1194	(*39*)
ethyl hexanoate	123-66-0	209	Sigma-Aldrich	99	144.21	2.83	88	1	8.359	1233	1238	(*39*)
hexyl acetate	142-92-7	213	Aldrich	99	144.21	2.83	43	1	9.323	1272	1269	(*39*)
anisole	100-66-3	2216	Aldrich	99.7	108.14	2.13	108	1	10.944	1337	1355	(*39*)
1-hexanol	111-27-3	20036	Sigma-Aldrich	99.9	102.17	1.94	56	1	11.468	1357	1354	(*39*)
ethyl octanoate	106-32-1	22	Aldrich	99	172.26	3.90	88	4	13.416	1435	1438	(*39*)
2-isobutyl-3-methoxy-pyrazine	24683-00-9	209	Pyrazine Specialties	99	166.22	2.61	124	2	15.610	1525	1527	(*39*)
linalool	78-70-6	2064	Merck	98	154.25	3.28	71	4	16.230	1551	1554	(*39*)
ethyl decanoate	110-38-3	21	Aldrich	99	200.32	4.96	88	2	18.309	1640	1647	(*39*)
ethyl benzoate	93-89-0	251	Aldrich	99	150.17	2.73	105	4	18.775	1660	1654	(*41*)
nerol	106-25-2	2014	Sigma-Aldrich	97+	154.25	3.28	93	2	21.910	1802	1793	(*42*)
2-phenylethyl acetate	103-45-7	2212	Aldrich	99	164.20	2.30	91	2	22.079	1810	1809	(*36*)
β-damascenone	23726-93-4	226	SAFC Supply Solution	1.1−1.3 (in ethanol)	190.28	4.04	69	2	22.212	1816	1820	(*42*)
α-ionone	127-41-3	217	Aldrich	90	192.30	3.86	121	2	22.827	1845	1840	(*40*)
phenylethyl alcohol	60-12-8	20206	Sigma	99	122.16	1.36	104	4	24.080	1906	1903	(*42*)
β-ionone	79-77-6	210	Sigma-Aldrich	95+	192.30	3.85	177	2	24.632	1933	1932	(*42*)
eugenol	97-53-0	2224	Aldrich	99	164.20	2.20	164	2	28.952	2149	2167	(*42*)

[a] Manufacturers: Aldrich, Milwaukee, WI; Sigma-Aldrich, St. Louis, MO; Sigma, St. Louis, MO; SAFC Supply Solution, St. Louis, MO; Merck, Darmstadt, Germany; Pyrazine Specialties, Atlanta, GA. [b] Log D: distribution coefficient at pH 3.0 and 25 °C calculated using Advanced Chemistry Development (ACD/Laboratories) software V8.14 for Solaris (1994−2009 ACD/Laboratories). [c] Cluster: compounds that respond similarly to optimization parameters determined by hierarchal cluster analysis as described under Experimental Procedures. [d] Unique ion (m/z): used for peak area determination. [e] RI: retention indices calculated from C8−C20 *n*-alkanes. [f] RI: retention indices reported in the literature for polyethylene glycol (PEG) capillary GC columns.

(14% vol vol^{-1}), glucose (240 g L^{-1}), glycerol (10 g L^{-1}), proline (2 g L^{-1}), catechin (50 mg L^{-1}), and their interactions on volatile partitioning. The concentrations used were intended to reflect the higher concentration ranges reported in *Vitis vinifera* grapes and table wines (*46*−*50*). The results were analyzed using a five-way ANOVA testing the effects of ethanol, glucose, glycerol, proline, catechin, and all two-way interactions. Least-squares (LS) means of peak area relative to the mean peak area observed in the water matrix, ± the standard error (SE), were plotted for significant two-way interactions.

Influence of Ethanol Concentration. Ethanol is a major component of the wine matrix. An artificial matrix with ethanol concentrations of 10, 11, 12, 13, 14, 15, 16, 17, and 18% vol vol^{-1} was spiked with the volatile standard mix to observe if there was a clear difference in partitioning of volatile compounds at varied concentrations of ethanol. Peak area was normalized to the average of that observed in Milli-Q water, and the results were analyzed using ANOVA. When values were significantly different, the bivariate data were fit to a linear-fit curve. A Student t test was used to test the significance of the curve slope for each volatile compound.

Influence of Glucose Concentration. Glucose is a major component of the grape juice matrix. An artificial matrix with glucose at 160, 180, 200, 220, 240, 260, 280, 300, or 320 g L^{-1} was spiked with the volatile standard mix designed to determine if glucose at typical juice concentrations influenced the partitioning of volatile compounds. Results were treated and analyzed in the same way as the ethanol concentration study.

Influence of Ethanol and Glucose on SPME Linearity. Quantitative SPME methodology commonly generates a standard calibration curve, using the optimized SPME extraction methodology, to determine the compound concentration from the sample peak area. To achieve this, compounds of interest are typically spiked, at known concentrations, into a model solution that reflects the sample matrix. Standard curves for the compounds in the volatile standard mix were generated in 240 g L^{-1} glucose and 14% vol vol^{-1} ethanol and compared to Milli-Q water to determine the slope of the calibration curves. Dilutions of the volatile standard mix were made to cover a 200-fold range in concentration. Results were treated and analyzed in the same way as for the ethanol concentration study.

Influence of Ethanol Concentration on Wine Volatile Partitioning. The ethanol concentrations of one red and one white wine were manipulated by dilution with ethanol and Milli-Q water to reflect the ethanol range of the synthetic wines. Although many compounds were identified in the wine samples, only a selection of 20 target compounds were analyzed as they were common between both wines. **Table 4** lists these target compounds. A number of compounds used in the standard volatile mix were not detectable in the wine samples. Peak area was multiplied by the dilution factor and normalized to the average of that observed in the undiluted wine sample. Wines were also diluted with a 14% vol vol^{-1} ethanol solution to compare the dilution effect while maintaining the ethanol concentration. Results were analyzed in the same way as for the ethanol concentration study.

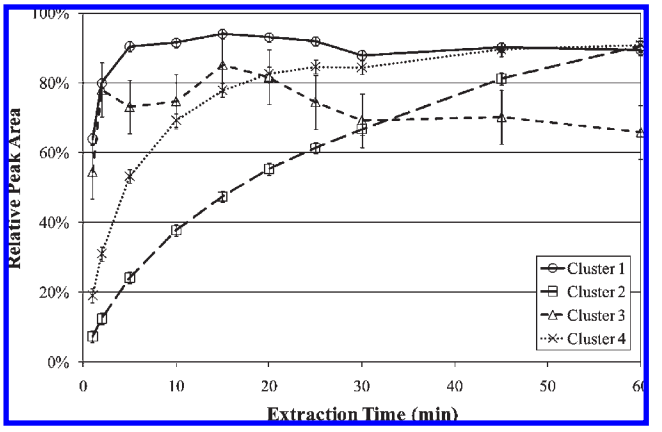

Figure 1. SPME extraction time optimization. Data points represent the LS means (±SE) for compounds belonging to clusters 1−4; please refer to **Table 1** for compound cluster membership. Peak areas are relative to the maximum peak area observed in the water matrix.

RESULTS AND DISCUSSION

Optimization of SPME Extraction Time. Figure 1 shows that peak area increased with increasing extraction time for all

Table 2. Significance Values for Standard Least-Squares Analysis of Variance for Main Effects of Catechin (CAT), Ethanol (ETH), Glucose (GLU), Glycerol (GLY), Proline (PRO), and All Two-Way Interactions[a]

compound	CAT	ETH	GLU	GLY	PRO	CAT × GLY	CAT × PRO	ETH × CAT	ETH × GLY	ETH × PRO	GLU × CAT	GLU × ETH	GLU × GLY	GLU × PRO	PRO × GLY
ethyl 2-methylbutyrate	0.325	***<0.001***	***<0.001***	0.806	0.433	***<0.001***	0.534	0.071	0.680	0.117	0.097	***<0.001***	0.485	0.742	0.161
ethyl 3-methylbutyrate	0.930	***<0.001***	***<0.001***	***0.021***	0.711	0.540	0.817	0.589	0.936	0.813	0.220	***<0.001***	***0.023***	0.921	0.104
isoamyl acetate	0.896	***<0.001***	***<0.001***	0.234	0.314	***<0.001***	0.629	0.143	0.265	0.217	0.091	***<0.001***	0.361	0.931	0.113
limonene	0.827	***<0.001***	0.505	0.793	0.352	0.530	0.172	0.819	0.687	0.262	0.675	0.072	0.562	0.858	0.334
ethyl hexanoate	0.469	***<0.001***	***<0.001***	0.663	0.219	***<0.001***	0.895	0.096	0.790	0.283	0.226	***<0.001***	0.581	0.740	0.473
hexyl acetate	0.505	***<0.001***	***<0.001***	0.892	0.554	***<0.001***	0.561	0.146	0.473	0.121	0.238	***<0.001***	0.760	0.929	0.542
anisole	0.366	***<0.001***	***<0.001***	0.668	0.134	***0.002***	0.584	0.106	0.524	0.193	0.176	***<0.001***	0.699	0.922	0.169
1-hexanol	0.066	***<0.001***	***<0.001***	***0.028***	0.730	0.271	0.301	0.167	0.082	0.313	0.061	***<0.001***	0.266	0.713	0.307
ethyl octanoate	0.457	***<0.001***	***<0.001***	0.531	0.578	***0.002***	0.438	0.618	0.561	0.650	0.183	***<0.001***	0.296	0.795	0.566
2-isobutyl-3-methoxypyrazine	0.064	***<0.001***	***<0.001***	***0.017***	0.140	***0.035***	0.196	0.543	***0.038***	0.795	0.369	***<0.001***	0.061	0.994	0.820
linalool	0.095	***<0.001***	***<0.001***	***0.002***	0.080	***0.038***	0.113	0.635	***0.008***	0.310	0.308	***<0.001***	0.104	0.439	0.844
ethyl decanoate	***0.020***	***<0.001***	***<0.001***	***0.027***	***0.033***	0.737	***0.031***	0.233	0.395	0.624	***0.009***	***0.008***	0.193	0.057	0.473
ethyl benzoate	0.199	***<0.001***	***<0.001***	***0.024***	0.060	***0.024***	0.245	0.922	0.053	0.656	0.363	***<0.001***	***0.043***	0.968	0.650
nerol	0.058	***<0.001***	***<0.001***	***<0.001***	0.218	0.090	0.093	0.797	***<0.001***	0.790	0.383	***<0.001***	0.343	0.341	0.437
2-phenylethyl acetate	***0.048***	***<0.001***	***<0.001***	***<0.001***	***0.041***	0.088	0.127	0.535	***0.002***	0.642	0.422	***<0.001***	***0.013***	0.766	0.831
β-damascenone	***0.046***	***<0.001***	***<0.001***	***0.003***	0.124	***0.032***	0.164	0.488	***0.006***	0.636	0.611	***<0.001***	0.122	0.954	0.821
α-ionone	***0.041***	***<0.001***	***<0.001***	***0.012***	0.324	***0.035***	0.365	0.674	***0.010***	0.428	0.643	***<0.001***	0.752	0.778	0.621
phenylethyl alcohol	***0.010***	***<0.001***	***<0.001***	0.093	***0.007***	0.839	0.166	0.636	0.116	0.768	0.490	***<0.001***	***0.005***	0.792	***0.047***
β-ionone	***0.039***	***<0.001***	***<0.001***	***0.042***	0.484	***0.045***	0.629	0.518	***0.016***	0.485	0.583	***<0.001***	0.726	0.755	0.465
eugenol	***0.014***	***<0.001***	***<0.001***	***<0.001***	0.177	0.087	0.202	0.805	***<0.001***	0.637	0.440	***<0.001***	0.267	0.990	0.696

[a] Values marked in bold italics are significant at $p \leq 0.05$.

compounds with the exception of limonene. Limonene was the only compound belonging to cluster 3, and its peak area was not significantly different between extraction times of 1 and 60 min. Compounds belonging to cluster 1 (please refer to **Table 1** for cluster membership) increased significantly to a maximum peak area at 5 min, whereas compounds belonging to cluster 4 showed no significant increase in peak area after 15−20 min. Compounds belonging to cluster 1 typically had lower molecular weights and eluted earlier in the chromatogram compared to compounds in clusters 2 and 4. Compounds belonging to cluster 2 increased steadily with increasing extraction time but did not appear to reach a maximum in the extraction time range assessed. It is likely that compounds belonging to cluster 2 are being refreshed from the solution as they are depleted from the headspace by the SPME fiber. These results are consistent with previous studies (*18*, *51*, *52*). An extraction time of 15 min was considered to be adequate to establish equilibrium between the fiber and the sample headspace, minimizing additional repartitioning from the solution to the headspace.

Interaction Effects of Major Grape and Wine Matrix Components. All compounds were influenced by one or more of the matrix components assessed (**Table 2**). Limonene was unique as it was significantly affected only by the presence of ethanol (**Table 2**). Proline was found to significantly influence three compounds; however, the magnitudes of these influences were approximately 1−2% (data not presented), indicating that it had no real effect.

All compounds, with the exception of limonene, were affected by glucose, ethanol, and the two-way interaction between glucose and ethanol. **Figure 2** shows that ethanol caused a reduction in relative peak area, whereas the presence of glucose resulted in an increase in relative peak area for all compounds. The combination of ethanol and glucose resulted in a slightly increased relative peak area when compared to ethanol in isolation; however, it is unlikely that both of these matrix components would be found together in table wines at the concentrations used. The magnitude of the ethanol effect was typically larger for the higher molecular weight compounds, in particular, the potent aroma compounds such as 2-isobutyl-3-methoxypyrazine, β-damascenone, α-ionone, and β-ionone, whereas the magnitude of the glucose effect was unrelated to molecular weight.

Significant two-way interactions were observed between ethanol and glycerol (**Table 2**) for 2-isobutyl-3-methoxypyrazine, linalool, nerol, 2-phenylethyl acetate, β-damascenone, α-ionone, β-ionone, and eugenol. **Figure 3** reiterates the observation that ethanol plays an important role in reducing relative peak area but also shows that glycerol can significantly increase the relative peak area in the absence of ethanol. Glycerol has no significant effect in the presence of ethanol, and it is unlikely that both of these matrix components would be found in isolation at the concentrations used because they are both products of yeast primary metabolism. Two previous studies have concluded that glycerol, in the range of 5−50 g L^{-1} in aqueous ethanol, had no impact on volatile partitioning, which is consistent with the results of this experiment (*53*, *54*). Furthermore, increasing the glycerol content of Chardonnay wine was found not to change the overall flavor perception (*54*). As such, glycerol is not likely to have a significant role in the volatile partitioning of aroma compounds in wine.

Significant two-way interactions were observed between catechin and glycerol for a number of compounds (**Table 2**); however, there were mixed effects. Ethyl-2-methylbutyrate, isoamyl acetate, ethyl hexanoate, hexyl acetate, anisole, and ethyl octanoate had significantly higher relative peak areas with either glycerol or catechin compared to neither glycerol nor catechin or both glycerol and catechin (**Figure 4**). Solutions with glycerol had significantly higher relative peak areas for 2-isobutyl-3-methoxypyrazine, linalool, ethyl benzoate, β-damascenone, α-ionone, and β-ionone compared to solutions without glycerol or if there were glycerol with catechin. Previous research has indicated that catechin, at concentrations between 0 and 5 g L^{-1}, reduced the relative activity coefficient of benzaldehyde, isoamyl acetate, and ethyl hexanoate by ∼5−10% (*55*). In that previous study, nuclear magnetic

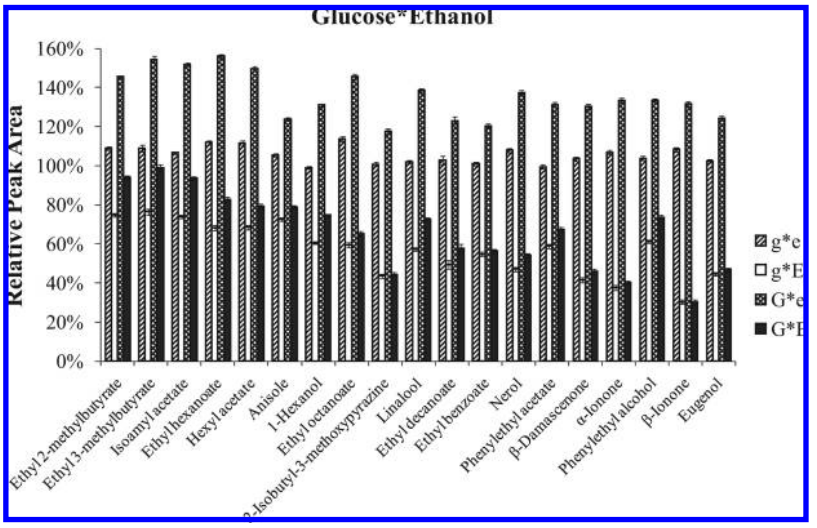

Figure 2. Compounds significantly influenced by an interaction between glucose and ethanol. Data points represent the LS means of peak area relative to the mean peak area observed in the water matrix (±SE). Capital letters denote the presence of the matrix component, whereas lower case letters denote the absence; G corresponds to glucose, and E corresponds to ethanol.

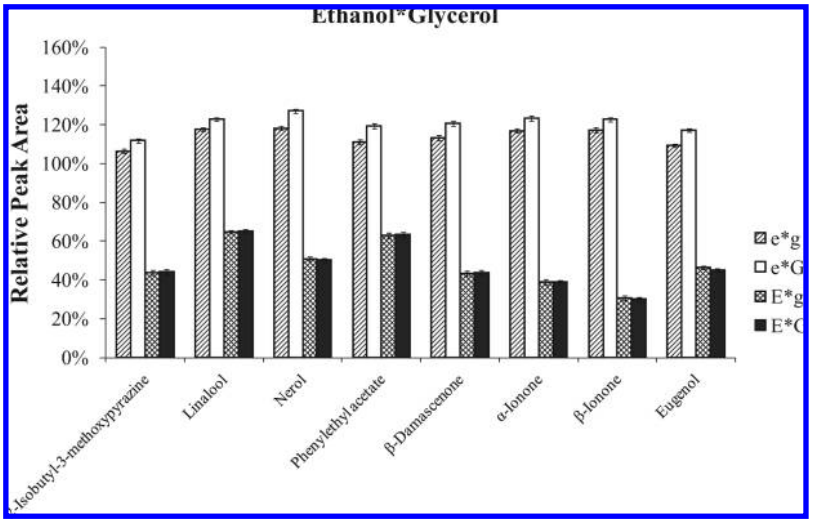

Figure 3. Compounds significantly influenced by an interaction between ethanol and glycerol. Data points represent the LS means of peak area relative to the mean peak area observed in the water matrix (±SE). Capital letters denote the presence of the matrix component, whereas lower case letters denote the absence; E corresponds to ethanol, and G corresponds to glycerol.

resonance (NMR) spectroscopy was used to determine that the relative activity coefficient reduction in the presence of catechin was caused by hydrophobic aroma−phenolic interactions. Gallic acid has also been shown to reduce the partitioning and perceived aroma intensity of 2-methylpyrazine (*56*), which has been attributed to increased $\pi-\pi$ stacking between the galloyl ring and the aromatic ring of the aroma compounds (*57*). The results presented in **Figure 4** neither reaffirm nor disprove these previous observations. The magnitude of the effect for the catechin and glycerol interaction was 4−7%, diminishing the importance of this matrix interaction as compared to the effect of ethanol and glucose presented in **Figure 2**. The reduced impact of catechin compared to previous research could be attributed to the significantly lower concentration used in this study and the addition of other matrix components, which may change the intermolecular interactions of catechin. However, it is difficult to explain the causative nature of the matrix interactions between glycerol and catechin, and further research is warranted to better understand the role of wine phenolic compounds in aroma−phenolic interactions.

Influence of Ethanol Concentration. Increasing concentrations of ethanol decreased the relative peak area for all compounds (**Table 3**). Previous HS-SPME optimization studies assessing aqueous ethanol model solutions and alcoholic beverages have indicated that ethanol reduces the efficiency of HS-SPME (*9*, *58*, *59*). It has been suggested that this reduced efficiency is due to ethanol directly competing with analytes for SPME binding sites (*60*−*62*). However, SHS methods have been used effectively to determine partition coefficients of analytes in aqueous ethanol solutions (*19*−*21*). One study compared phase ratio variation (PRV), vapor phase calibration (VPC), and liquid calibration static headspace (LC-SH) SHS methods and showed that regardless of which SHS method was employed, increasing ethanol concentration in solution leads to lower partition coefficients for ethyl hexanoate and isoamyl alcohol (*20*). This study did not utilize SHS as it is a less sensitive and less selective method for headspace analysis compared to SPME (*63*), and with the

Table 3. Linear Fit Slope Values Reflecting the Percentage Change (± SE) in Peak Area (Relative to the Average Peak Area Measured in the Water Matrix) per 1.0% vol vol^{-1} Change in Ethanol (over the Range 10−18% Ethanol), 10 g L^{-1} Change in Glucose (over the Range 160−320 g L^{-1}), and 200-fold Change in Analyte Concentration in 14% Ethanol, 240 g L^{-1} Glucose, and Milli-Q Water, Respectively[a]

	linear fit slope (analyte)		linear fit slope (Δ analyte)		
compound	Δ ethanol	Δ glucose	ethanol	glucose	H_2O
ethyl 2-methylbutyrate	***−2.01 ± 0.15***	***0.66 ± 0.19***	***58.83 ± 0.67***	***129.69 ± 3.71***	***98.61 ± 1.76***
ethyl 3-methylbutyrate	***−2.35 ± 0.15***	***1.54 ± 0.37***	***62.86 ± 1.13***	***132.37 ± 4.85***	***97.95 ± 3.05***
isoamyl acetate	***−2.46 ± 0.16***	***0.69 ± 0.29***	***61.48 ± 0.69***	***129.04 ± 3.82***	***98.31 ± 2.38***
limonene	***−2.21 ± 1.03***	−0.59 ± 0.91	***75.09 ± 1.21***	***89.90 ± 3.51***	***99.07 ± 2.74***
ethyl hexanoate	***−2.85 ± 0.24***	0.14 ± 0.35	***52.09 ± 0.47***	***139.76 ± 1.96***	***99.18 ± 1.77***
hexyl acetate	***−2.78 ± 0.24***	0.13 ± 0.33	***53.88 ± 0.41***	***136.95 ± 2.30***	***99.05 ± 1.86***
anisole	***−2.53 ± 0.20***	0.25 ± 0.19	***62.09 ± 0.49***	***115.43 ± 2.05***	***99.41 ± 1.35***
1-hexanol	***−2.06 ± 0.13***	***1.34 ± 0.12***	***52.81 ± 0.46***	***127.35 ± 3.53***	***98.63 ± 2.04***
ethyl octanoate	***−3.07 ± 0.25***	−0.15 ± 0.53	***42.57 ± 0.34***	***122.61 ± 0.54***	***99.59 ± 0.73***
2-isobutyl-3-methoxypyrazine	***−3.07 ± 0.24***	−0.16 ± 0.31	***38.81 ± 0.54***	***110.96 ± 1.98***	***99.73 ± 1.85***
linalool	***−2.63 ± 0.22***	***0.8 ± 0.25***	***51.42 ± 0.52***	***131.98 ± 3.14***	***99.2 ± 1.84***
ethyl decanoate	***−2.69 ± 0.27***	−0.27 ± 0.52	***40.71 ± 0.35***	***97.82 ± 3.66***	***99.28 ± 2.50***
ethyl benzoate	***−3.19 ± 0.28***	−0.11 ± 0.30	***48.72 ± 0.61***	***113.21 ± 2.10***	***99.58 ± 1.67***
nerol	***−2.29 ± 0.40***	0.03 ± 0.21	***39.23 ± 0.36***	***128.46 ± 1.13***	***100.15 ± 0.49***
2-phenylethyl acetate	***−2.87 ± 0.33***	0.54 ± 0.36	***55.05 ± 0.70***	***126.15 ± 2.40***	***99.67 ± 1.77***
β-damascenone	***−3.35 ± 0.31***	−0.27 ± 0.38	***37.19 ± 0.63***	***121.45 ± 1.97***	***100.23 ± 1.63***
α-ionone	***−3.38 ± 0.29***	−0.40 ± 0.32	***32.50 ± 0.61***	***119.55 ± 1.32***	***100.23 ± 1.40***
phenylethyl alcohol	***−2.51 ± 0.27***	***1.07 ± 0.14***	***52.79 ± 0.68***	***124.55 ± 1.80***	***99.25 ± 1.31***
β-ionone	***−3.30 ± 0.24***	−0.58 ± 0.29	***25.66 ± 0.54***	***115.64 ± 1.13***	***100.42 ± 1.35***
eugenol	***−3.21 ± 0.37***	0.11 ± 0.23	***41.77 ± 0.63***	***124.04 ± 2.95***	***100.43 ± 1.88***

[a] Linear Fit Slope values marked in bold italics are significant at $p \leq 0.05$.

increasing use of SPME as a routine automated technique, we felt that HS-SPME would be a useful technique for studying the interactions between volatile compounds and the nonvolatile matrix components.

The effect of increasing ethanol was particularly pronounced for 2-isobutyl-3-methoxypyrazine, β-damascenone, α-ionone, and β-ionone, which had relative peak areas of 46, 49, 45, and 37%, respectively, at 14% ethanol vol vol^{-1}, compared to water. Whiton and Zoecklein found that ethyl acetate, ethyl hexanoate, hexyl acetate, ethyl decanoate, 2-phenylethyl alcohol, 4-ethylguaiacol, and 4-ethylphenol showed a decrease of 20−30%, with β-ionone decreasing by nearly 50% between 11 and 14% ethanol (*59*). In a more recent study, Câmara and co-workers observed that 12% ethanol vol vol^{-1} decreased the peak area (relative to the octan-3-ol internal standard) of β-ionone, β-damascenone, and α-ionone by ∼40, 60, and 30%, respectively (*9*). The actual change in relative peak area would be significantly larger than this as it is expected that the octan-3-ol internal standard would also be affected by the change in ethanol concentration. It is also difficult to ascertain if the observed effect of ethanol in these two studies also reflects the addition of sodium chloride to the matrix, which is known to significantly weaken the water−ethanol hydrogen-bonding structure (*64*). The recent use of an in-fiber standard, which is loaded directly into the SPME fiber coating prior to the sample extraction step, has been successfully used to correct for matrix effects (*18*, *65*−*67*) and may be a useful solution in qualitative or semiquantitative analysis for comparing samples with varied ethanol content.

For each analyte, increasing ethanol in the matrix was negatively correlated with analyte peak area and was linear over the range 10−18% vol vol^{-1}. **Table 3** lists the slope values for relative peak area with slope values ranging from −2.01% for ethyl-2-methylbutyrate to −3.38 for α-ionone. Previous studies have observed that the magnitude of the ethanol effect is positively correlated with the partition coefficient (*68*) due to a cosolvent effect of ethanol (*53*). It is clear from the results presented here and from previous studies that ethanol plays a significant and important role in the headspace partitioning of volatile compounds.

Influence of Glucose Concentration. Glucose increased the measured headspace peak area for most compounds; however, there was no clear linear trend between 160 and 320 g L^{-1} with the exception of ethyl-2-methylbutyrate, ethyl-3-methylbutyrate, isoamyl acetate, 1-hexanol, linalool, and phenylethyl alcohol (**Table 3**). The magnitude of these trends was not as large as was found for ethanol. A previous study observed that increasing solution viscosity using sucrose from 12.7 and 156 mPa s^{-1} reduced volatile compound release from solution due to reduced mass transfer of volatile compounds (*69*). However, sucrose was found to have a larger effect than carboxymethylcellulose and guar gum at similar levels of viscosity, indicating that sucrose exhibited both viscosity and binding interactions at the concentrations used.

The viscosity of the glucose solutions used in the current study ranged from 1.5 to 2.3 mPa s^{-1}, calculated from eq 1, relative to 1.0 mPa s^{-1} for water (*70*). Thus, reduced volatile release due to viscosity would not be expected in this study. Viscosity calculation for sugar solutions from Chirife and Buera (*70*) is shown in eq 1

$$\mu_r = a\, e^{EM/55.51+M} \quad (1)$$

where μ_r is the relative viscosity, α and E are constants (glucose at 20 °C: α = 0.954, E = 27.93), and M is the number of moles of glucose.

Other studies have identified that increasing sugar concentration, within the range typical of grape juice, increases the headspace partitioning of volatile compounds with no viscosity effect (*71*, *72*). Another study assessed 40 volatiles from different chemical classes and observed that some compounds increased, others decreased, and some remained unchanged with increasing sucrose concentration (*73*). The changes in volatile headspace concentrations were analyzed using partial least-squares (PLS) regression analysis to find that the square of the log of the partition coefficient [(log P)^2], lowest unoccupied molecular orbital (LUMO) energy, and a first-order connectivity index term were the most important descriptors for explaining the change in volatility due to increased sucrose concentration (*73*).

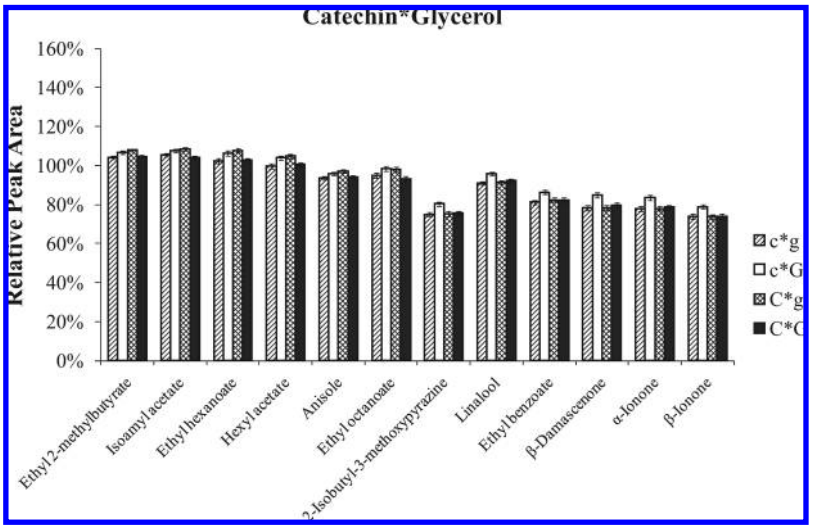

Figure 4. Compounds significantly influenced by an interaction between catechin and glycerol. Data points represent the LS means of peak area relative to the mean peak area observed in the water matrix (±SE). Capital letters denote the presence of the matrix component, whereas lower case letters denote the absence; C corresponds to catechin, and G corresponds to glycerol.

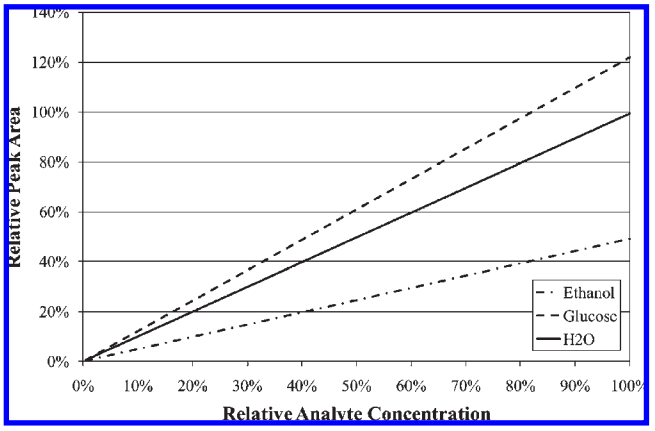

Figure 5. Model of the effect of ethanol and glucose on relative peak area. Linear curves reflect the average slope value for compounds listed in **Table 3** over a 200-fold change in analyte concentration in 14% ethanol, 240 g L^{-1} glucose, and Milli-Q water, respectively.

The results of the current study suggest that direct comparisons can be made between different juices using qualitative volatile analysis without taking into account the glucose concentration within the range 160−320 g L^{-1}.

Influence of Ethanol and Glucose on SPME Linearity. All compounds showed a positive linear trend with respect to relative peak area and solution concentration; however, the slopes associated with glucose and ethanol solutions were distinctly different from that in water (**Figure 5**). Slope values for varied volatile concentrations in the 14% vol vol^{-1} ethanol solution ranged from 75.09 for limonene to 25.66 for β-ionone; however, the next highest value was 62.86 for ethyl-3-methylbutyrate (**Table 3**). Slope values for varied volatile concentrations in the 240 g L^{-1} glucose solution varied from 89.90 for limonene to 139.76 for ethyl hexanoate and were typically >100 with the exception of limonene and ethyl decanoate; however, that for ethyl decanoate was close to 100 (**Table 3**). This clearly indicates that it is absolutely essential to develop calibration curves in model ethanol or glucose solutions that reflect the samples to be assessed when quantitative analysis of volatiles in juices or alcoholic beverages is conducted using SPME.

Influence of Ethanol Concentration on Wine Volatile Partitioning. The wine headspace volatiles studied included a large number of compounds; however, a set of 20 compounds common to both the white and red wines were assessed. The SPME methodology was not sensitive enough to detect a number of compounds that were included in the initial synthetic studies; however, ethyl-2-methylbutyrate, ethyl-3-methylbutyrate, isoamyl acetate, ethyl hexanoate, hexyl acetate, 1-hexanol, ethyl octanoate, ethyl decanoate, 2-phenylethyl acetate, and phenylethyl alcohol were common to the previous synthetic studies. Analysis of variance showed that there was a significant difference between different ethanol concentrations for all compounds, similar to that observed in the model solutions. Subsequent linear regression analysis showed that all compounds, with the exception of isobutanol, decreased with the addition of ethanol and increased with the addition of water. This is consistent with the observations of Conner et al. (*19*), who reported that increasing the ethanol concentration in aqueous ethanol solutions increases the solubility of esters in solution and reduces the headspace concentration. The results suggest that the matrix is affecting the partitioning of analytes into the headspace of the sample vial. Headspace analysis using SPME can be best understood by using the three-phase system equilibrium as proposed by Zhang and Pawliszyn (*5*). The HS-SPME three-phase equilibrium equation (*5*) is given by eq 2

$$n = \frac{C_0 V_1 V_2 K_{h/f} K_{s/h}}{(K_{h/f} K_{s/h} V_1) + (K_{s/h} V_3) + V_3} \quad (2)$$

where n is the mass of any one analyte absorbed to the fiber, C_0 is the initial analyte concentration in solution, V_1 is the volume of SPME phase, V_2 is the liquid volume, V_3 is the headspace volume, $K_{s/h}$ is the sample/headspace partition coefficient, and $K_{h/f}$ is the headspace/fiber partition coefficient. When V_1, V_2, V_3, and $K_{h/f}$ are kept constant, this relationship can be simplified to eq 3, the relationship between analyte concentration in solution and $K_{s/h}$:

$$\Delta(C_0 K_{s/h}) \propto \Delta n \quad (3)$$

The data presented in **Table 4** clearly demonstrate that increasing the ethanol concentration of either a red or white wine results in a linear decrease in volatile compound concentration in the headspace. The model proposed in eq 3 suggests that if $K_{s/h}$ for

Table 4. Volatile Compounds Identified in Wine Used for the Characterisation of Ethanol Effects on Volatile Partitioning

						RI			linear fit slope[e]	
compound	CAS Registry No.	MW	Log *D*[a]	unique ion[b]	RT (min)	calcd[c]	lit.[d]	ref (lit.)	white	red
ethyl 2-methylbutyrate	7452-79-1	130.18	2.12	102	4.378	1046	1056	(*40*)	***−2.58 ± 0.50***	***−3.59 ± 0.37***
ethyl 3-methylbutyrate	108-64-5	130.18	2.12	88	4.644	1061	1068	(*39*)	***−2.19 ± 0.49***	***−3.54 ± 0.45***
isobutanol	78-83-1	74.12	0.69	43	5.351	1102	1097	(*39*)	1.16 ± 1.02	−1.91 ± 1.24
isoamyl acetate	123-92-2	130.18	2.12	43	5.650	1115	1125	(*39*)	***−2.01 ± 0.80***	***−3.57 ± 0.55***
isoamyl alcohol	123-51-3	88.15	1.22	55	7.838	1212	1215	(*39*)	***−1.38 ± 0.41***	***−2.70 ± 0.48***
ethyl hexanoate	123-66-0	144.21	2.83	88	8.292	1230	1238	(*39*)	***−3.07 ± 0.41***	***−4.01 ± 0.56***
hexyl acetate	142-92-7	144.21	2.83	43	9.239	1269	1269	(*39*)	***−3.00 ± 0.46***	***−2.75 ± 0.62***
ethyl lactate	97-64-3	88.15	1.22	45	11.037	1340	1353	(*37*)	***−0.73 ± 0.20***	***−0.71 ± 0.14***
1-hexanol	111-27-3	102.17	1.94	56	11.412	1355	1354	(*39*)	***−2.08 ± 0.52***	***−3.59 ± 0.48***
methyl octanoate	111-11-5	158.24	3.37	74	12.204	1387	1387	(*39*)	***−3.03 ± 0.52***	***−4.32 ± 0.57***
ethyl octanoate	106-32-1	172.26	3.90	88	13.453	1437	1438	(*39*)	***−3.61 ± 0.33***	***−4.82 ± 0.45***
vitispirane	65416-59-3	192.30	3.81	192	15.514	1521	1507	(*38*)	***−3.72 ± 0.40***	***−4.33 ± 0.43***
1-octanol	111-87-5	130.23	3.00	56	16.444	1560	1561	(*39*)	***−2.03 ± 0.75***	***−4.64 ± 0.48***
ethyl decanoate	110-38-3	200.32	4.96	88	18.331	1641	1647	(*39*)	***−3.67 ± 0.26***	***−6.40 ± 0.31***
diethyl succinate	123-25-1	174.19	1.26	101	19.078	1673	1690	(*37*)	***−3.04 ± 0.45***	***−3.63 ± 0.48***
ethyl 9-decenoate	67233-91-4	198.30	4.45	88	19.435	1689	1694	(*37*)	***−3.36 ± 0.47***	***−6.82 ± 0.42***
TDN	30364-38-6	172.27	4.92	157	20.430	1734	1719	(*38*)	***−4.55 ± 0.34***	***−4.28 ± 0.42***
2-phenylethyl acetate	103-45-7	164.20	2.30	91	22.017	1807	1809	(*36*)	***−3.46 ± 0.46***	***−4.85 ± 0.54***
isoamyl decanoate	2306-91-4	242.40	6.37	70	23.144	1861	1853	(*38*)	***−7.70 ± 0.68***	***−6.66 ± 0.64***
phenylethyl alcohol	60-12-8	122.16	1.36	104	24.024	1903	1903	(*42*)	***−4.15 ± 0.65***	***−3.80 ± 0.44***

[a] Log *D*: distribution coefficient at pH 3.0 and 25 °C calculated using Advanced Chemistry Development (ACD/Laboratories) software V8.14 for Solaris (1994−2009 ACD/Laboratories). [b] Unique ion (*m*/*z*): used for peak area determination. [c] RI: retention indices calculated from C8−C20 *n*-alkanes. [d] RI: retention indices reported in the literature for polyethylene glycol (PEG) capillary GC columns or equivalent. [e] Linear fit slope values reflecting the percentage change (±SE) in peak area (relative to the average peak area measured in the 14% ethanol red and white wines, respectively) per 1.0% change in ethanol (over the range 10−18% ethanol). Linear fit slope values marked in bold italics are significant to $p \leq 0.05$.

any one analyte remained constant, then a decrease in analyte concentration in solution after dilution would result in a proportional decrease in the mass of compound released into the headspace and consequently absorbed to the SPME fiber. This is not observed; rather, dilution with ethanol results in a significant decrease, whereas dilution with water results in a significant increase for all analytes with the exception of isobutanol (data not presented). As a consequence, the observed change in relative abundance absorbed to the fiber is likely to be dependent on the solubility of each compound in solution.

Table 4 shows the relative slope values for the linear fit curve. This is consistent with the results of the model solution studies above; however, it was interesting to note that the slope values were typically larger for the same compounds found in red wine compared to the model ethanol solutions or the white wine (**Figure 6**). This highlights that ethanol may interact with other major wine components that are present in the red wine and not present in the white wine to influence volatile partitioning.

A recent study has identified that the odor threshold (OT) for β-damascenone in red wine was 7000 ng L^{-1}, or 1000-fold higher compared to an OT of 50 ng L^{-1} in aqueous ethanol (*33*). Another recent study suggests that the OT for this compound in water is 13 ng L^{-1}, compared to 2 ng L^{-1} which is the most frequently referenced OT (*34*), with the recognition threshold of 56 ng L^{-1} (*74*). Comparison of both studies highlights that it is difficult to accurately determine OT for specific compounds and that distinct differences in OT values can be attributed to interactions with the major wine components. Although the results of the current study do not show a reduction in headspace concentration of this magnitude, the results indicate that the wine matrix, in particular, the wine ethanol concentration, has a direct impact on the headspace abundance due to changes associated with the compound-specific $K_{s/h}$.

The results presented indicate that the wine matrix, in particular, the wine ethanol concentration, has a direct impact on the solubility of wine volatile compounds and subsequently affects the headspace abundance due to changes associated with the compound-specific $K_{s/h}$. It is likely that the matrix influence on the compound-specific partition coefficient significantly affects the partitioning of aroma compounds into the headspace and therefore changes their aroma impact. These findings help to explain recent observations by other research groups assessing the sensory impact of wine volatiles. A distinction of this study is that it characterized a number of wine matrix interaction effects demonstrating that ethanol plays an important and significant role in volatile partitioning. Further studies into this phenomenon are warranted to better elucidate how the solution matrix changes the aroma perception of complex mixtures.

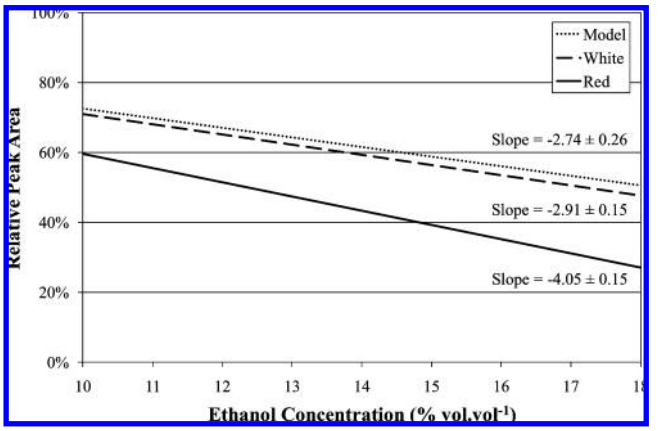

Figure 6. Model of the effect of ethanol concentration on relative peak area. Linear curves reflect the average slope value for the compounds assessed in model solution (**Table 3**), white and red wines (**Table 4**) (±SE).

LITERATURE CITED

(1) Plug, H.; Haring, P. The influence of flavour−ingredient interactions on flavour perception. *Food Qual. Pref.* **1994**, *5* (1−2), 95–102.

(2) McNaught, A. D.; Wilkinson, A. *Compendium of Chemical Terminology: IUPAC Recommendations* (*The Gold Book*), 2nd ed.; Blackwell Science: Oxford, U.K., 1997.
(3) Arthur, C. L.; Pawliszyn, J. Solid phase microextraction with thermal desorption using fused silica optical fibers. *Anal. Chem.* **1990**, *62*, 2145–2148.
(4) Arthur, C. L.; Killam, L. M.; Buchholz, K. D.; Pawliszyn, J.; Berg, J. R. Automation and optimization of solid-phase microextraction. *Anal. Chem.* **1992**, *64*, 1960–1966.
(5) Zhang, Z.; Pawliszyn, J. Headspace solid-phase microextraction. *Anal. Chem.* **1993**, *65*, 1843–1852.
(6) Pan, L.; Adams, M.; Pawliszyn, J. Determination of fatty acids using solid-phase microextraction. *Anal. Chem.* **1995**, *67*, 4396–4403.
(7) Steffen, A.; Pawliszyn, J. Analysis of flavor volatiles using headspace solid-phase microextraction. *J. Agric. Food Chem.* **1996**, *44*, 2187–2193.
(8) Siebert, T. E.; Smyth, H. E.; Capone, D. L.; Neuwöhner, C.; Pardon, K. H.; Skouroumounis, G. K.; Herderich, M. J.; Sefton, M. A.; Pollnitz, A. P. Stable isotope dilution analysis of wine fermentation products by HS-SPME-GC-MS. *Anal. Bioanal. Chem.* **2005**, *381* (4), 937–947.
(9) Câmara, J. S.; Alves, M. A.; Marques, J. C. Development of headspace solid-phase microextraction−gas chromatography−mass spectrometry methodology for analysis of terpenoids in Madeira wines. *Anal. Chim. Acta* **2006**, *555* (2), 191–200.
(10) Hartmann, P. J.; McNair, H. M.; Zoecklein, B. W. Measurement of 3-alkyl-2-methoxypyrazine by headspace solid-phase microextraction in spiked model wines. *Am. J. Enol. Vitic.* **2002**, *53* (4), 285–288.
(11) Mestres, M.; Marti, M. P.; Busto, O.; Guasch, J. Simultaneous analysis of thiols, sulphides and disulphides in wine aroma by headspace solid-phase microextraction−gas chromatography. *J. Chromatogr., A* **1999**, *849* (1), 293–297.
(12) Mestres, M.; Sala, C.; Marti, M. P.; Busto, O.; Guasch, J. Headspace solid-phase microextraction of sulphides and disulphides using Carboxen-polydimethylsiloxane fibers in the analysis of wine aroma. *J. Chromatogr., A* **1999**, *835* (1−2), 137–144.
(13) Carrillo, J. D.; Garrido-López, A.; Tena, M. T. Determination of volatile oak compounds in wine by headspace solid-phase microextraction and gas chromatography−mass spectrometry. *J. Chromatogr., A* **2006**, *1102* (1−2), 25–36.
(14) Sala, C.; Mestres, M.; Marti, M. P.; Busto, O.; Guasch, J. Headspace solid-phase microextraction method for determining 3-alkyl-2-methoxypyrazines in musts by means of polydimethylsiloxane-divinylbenzene fibres. *J. Chromatogr., A* **2000**, *880* (1−2), 93–99.
(15) Rocha, S.; Ramalheira, V.; Barros, A.; Delgadillo, I.; Coimbra, M. A. Headspace solid phase microextraction (SPME) analysis of flavor compounds in wines. Effect of the matrix volatile composition in the relative response factors in a wine model. *J. Agric. Food Chem.* **2001**, *49*, 5142–5151.
(16) Silva Ferreira, A. C.; Guedes De Pinho, P. Analytical method for determination of some aroma compounds on white wines by solid phase microextraction and gas chromatography. *J. Food Sci.* **2003**, *68* (9), 2817–2820.
(17) Howard, K. L.; Mike, J. H.; Riesen, R. Validation of a solid-phase microextraction method for headspace analysis of wine aroma components. *Am. J. Enol. Vitic.* **2005**, *56* (1), 37–45.
(18) Setkova, L.; Risticevic, S.; Pawliszyn, J. Rapid headspace solid-phase microextraction−gas chromatographic−time-of-flight mass spectrometric method for qualitative profiling of ice wine volatile fraction. I. Method development and optimization. *J. Chromatogr., A* **2007**, *1147* (2), 213–223.
(19) Conner, J. M.; Birkmyre, L.; Paterson, A.; Piggott, J. R. Headspace concentrations of ethyl esters at different alcoholic strengths. *J. Sci. Food Agric.* **1998**, *77* (1), 121–126.
(20) Athès, V.; Peña, Y; Lillo, M.; Bernard, C.; Pérez-Correa, R.; Souchon, I. Comparison of experimental methods for measuring infinite dilution volatilities of aroma compounds in water/ethanol mixtures. *J. Agric. Food Chem.* **2004**, *52*, 2021–2027.
(21) Conner, J. M.; Paterson, A.; Piggott, J. R. Interactions between ethyl esters and aroma compounds in model spirit solutions. *J. Agric. Food Chem.* **1994**, *42*, 2231–2234.
(22) Grosch, W. Evaluation of the key odorants of foods by dilution experiments, aroma models and omission. *Chem. Senses* **2001**, *26* (5), 533–545.
(23) Escudero, A.; Campo, E.; Fariña, L.; Cacho, J.; Ferreira, V. Analytical characterization of the aroma of five premium red wines. Insights into the role of odor families and the concept of fruitiness of wines. *J. Agric. Food Chem.* **2007**, *55*, 4501–4510.
(24) Le Berre, E.; Atanasova, B.; Langlois, D.; Etiévant, P.; Thomas-Danguin, T. Impact of ethanol on the perception of wine odorant mixtures. *Food Qual. Pref.* **2007**, *18* (6), 901–908.
(25) Guth, H. Identification of character impact odorants of different white wine varieties. *J. Agric. Food Chem.* **1997**, *45*, 3022–3026.
(26) Guth, H. Comparison of different white wine varieties in odor profiles by instrumental analysis and sensory studies. *ACS Symp. Ser.* **1998**, *No. 714*, 39–52.
(27) Kotseridis, Y.; Baumes, R. Identification of impact odorants in Bordeaux red grape juice, in the commercial yeast used for its fermentation, and in the produced wine. *J. Agric. Food Chem.* **2000**, *48*, 400–406.
(28) Ferreira, V.; Aznar, M.; López, R.; Cacho, J. Quantitative gas chromatography−olfactometry carried out at different dilutions of an extract. Key differences in the odor profiles of four high-quality Spanish aged red wines. *J. Agric. Food Chem.* **2001**, *49*, 4818–4824.
(29) Ferreira, V.; Ortín, N.; Escudero, A.; López, R.; Cacho, J. Chemical characterization of the aroma of Grenache rosé wines: aroma extract dilution analysis, quantitative determination, and sensory reconstitution studies. *J. Agric. Food Chem.* **2002**, *50*, 4048–4054.
(30) Escudero, A.; Gogorza, B.; Melús, M. A.; Ortín, N.; Cacho, J.; Ferreira, V. Characterization of the aroma of a wine from Maccabeo. Key role played by compounds with low odor activity values. *J. Agric. Food Chem.* **2004**, *52*, 3516–3524.
(31) Atanasova, B.; Thomas-Danguin, T.; Chabanet, C.; Langlois, D.; Nicklaus, S.; Etiévant, P. Perceptual interactions in odour mixtures: odour quality in binary mixtures of woody and fruity wine odorants. *Chem. Senses* **2005**, *30* (3), 209–217.
(32) Skouroumounis, G. K.; Sefton, M. A. The formation of β-damascenone in wine. In *Carotenoid-Derived Aroma Compounds*; Winterhalter, P. Rouseff, R., Eds.; American Chemical Society: Washington, DC, 2002; Vol. 802, pp 241−254.
(33) Pineau, B.; Barbe, J. C.; Van Leeuwen, C.; Dubourdieu, D. Which impact for β-damascenone on red wines aroma? *J. Agric. Food Chem.* **2007**, *55*, 4103–4108.
(34) Buttery, R. G.; Teranishi, R.; Ling, L. C.; Turnbaugh, J. G. Quantitative and sensory studies on tomato paste volatiles. *J. Agric. Food Chem.* **1990**, *38*, 336–340.
(35) Ward, J. H., Jr. Hierarchical grouping to optimize an objective function. *J. Am. Stat. Assoc.* **1963**, *58* (301), 236–244.
(36) Stein, S. E. An integrated method for spectrum extraction and compound identification from gas chromatography/mass spectrometry data. *J. Am. Soc. Mass Spectrom.* **1999**, *10* (8), 770–781.
(37) Lee, S. J.; Noble, A. C. Characterization of odor-active compounds in Californian Chardonnay wines using GC−olfactometry and GC−mass spectrometry. *J. Agric. Food Chem.* **2003**, *51*, 8036–8044.
(38) Selli, S.; Cabaroglu, T.; Canbas, A.; Erten, H.; Nurgel, C.; Lepoutre, J. P.; Gunata, Z. Volatile composition of red wine from cv. Kalecik Karasí grown in central Anatolia. *Food Chem.* **2004**, *85* (2), 207–213.
(39) Riu-Aumatell, M.; Bosch-Fusté, J.; López-Tamames, E.; Buxaderas, S. Development of volatile compounds of cava (Spanish sparkling wine) during long ageing time in contact with lees. *Food Chem.* **2006**, *95* (2), 237–242.
(40) Bianchi, F.; Careri, M.; Mangia, A.; Musci, M. Retention indices in the analysis of food aroma volatile compounds in temperature-programmed gas chromatography: database creation and evaluation of precision and robustness. *J. Sep. Sci.* **2007**, *30* (4), 563.
(41) Goodner, K. L. Practical retention index models of OV-101, DB-1, DB-5, and DB-Wax for flavor and fragrance compounds. *LWT−Food Sci. Technol.* **2008**, *41* (6), 951–958.
(42) Beck, J. J.; Higbee, B. S.; Merrill, G. B.; Roitman, J. N. Comparison of volatile emissions from undamaged and mechanically damaged almonds. *J. Sci. Food Agric.* **2008**, *88* (8), 1363–1368.

(43) Babushok, V. I.; Zenkevich, I. G. Retention indices for most frequently reported essential oil compounds in GC. *Chromatographia* **2009**, *69* (3−4), 257–269.
(44) Berg, H. W.; Keefer, R. M. Analytical determination of tartrate stability in wine. I. Potassium bitartrate. *Am. J. Enol. Vitic.* **1958**, *9* (4), 180–193.
(45) Lingane, J. J. Saturated potassium hydrogen tartrate solution as pH standard. *Anal. Chem.* **1947**, *19*, 810–811.
(46) Kliewer, W. M. The glucose−fructose ratio of *Vitis vinifera* grapes. *Am. J. Enol. Vitic.* **1967**, *18* (1), 33–41.
(47) Rankine, B. C.; Bridson, D. A. Glycerol in Australian wines and factors influencing its formation. *Am. J. Enol. Vitic.* **1971**, *22* (1), 6–12.
(48) Collins, T. S.; Miller, C. A.; Altria, K. D.; Waterhouse, A. L. Development of a rapid method for the analysis of ethanol in wines using capillary electrophoresis. *Am. J. Enol. Vitic.* **1997**, *48* (3), 280–284.
(49) Goldberg, D. M.; Karumanchiri, A.; Tsang, E.; Soleas, G. J. Catechin and epicatechin concentrations of red wines: regional and cultivar-related differences. *Am. J. Enol. Vitic.* **1998**, *49* (1), 23–34.
(50) Stines, A. P.; Naylor, D. J.; Høj, P. B.; Van Heeswijck, R. Proline accumulation in developing grapevine fruit occurs independently of changes in the levels of Δ^1-pyrroline-5-carboxylate synthetase mRNA or protein. *Plant Physiol.* **1999**, *120* (3), 923–931.
(51) Roberts, D. D.; Pollien, P.; Milo, C. Solid-phase microextraction method development for headspace analysis of volatile flavor compounds. *J. Agric. Food Chem.* **2000**, *48*, 2430–2437.
(52) Jung, D. M.; Ebeler, S. E. Headspace solid-phase microextraction method for the study of the volatility of selected flavor compounds. *J. Agric. Food Chem.* **2003**, *51*, 200–205.
(53) Fischer, C.; Fischer, U.; Jacob, L. Impact of matrix variables ethanol, sugar, glycerol, pH and temperature on the partition coefficients of aroma compounds in wine and their kinetics of volatilization. In *Proceedings for the 4th International Symposium on Cool Climate Viticulture and Enology*, Rochester, NY, July 16−20, 1996; Henick-Kling, T., Wolf, T. E., Harkness, E. M., Eds.; New York State Agricultural Experiment Station: Geneva, NY, 1996; pp 42−46.
(54) Lubbers, S.; Verret, C.; Voilley, A. The effect of glycerol on the perceived aroma of a model wine and a white wine. *Lebensm.-Wiss. -Technol.* **2001**, *34* (4), 262–265.
(55) Dufour, C.; Bayonove, C. L. Interactions between wine polyphenols and aroma substances. An insight at the molecular level. *J. Agric. Food Chem.* **1999**, *47*, 678–684.
(56) Aronson, J.; Ebeler, S. E. Effect of polyphenol compounds on the headspace volatility of flavors. *Am. J. Enol. Vitic.* **2004**, *55* (1), 13–21.
(57) Jung, D.-M.; de Ropp, J. S.; Ebeler, S. E. Study of interactions between food phenolics and aromatic flavors using one- and two-dimensional ^{1}H NMR spectroscopy. *J. Agric. Food Chem.* **2000**, *48*, 407–412.
(58) Mestres, M.; Busto, O.; Guasch, J. Headspace solid-phase microextraction analysis of volatile sulphides and disulphides in wine aroma. *J. Chromatogr., A* **1998**, *808* (1−2), 211–218.
(59) Whiton, R. S.; Zoecklein, B. W. Optimization of headspace solid-phase microextraction for analysis of wine aroma compounds. *Am. J. Enol. Vitic.* **2000**, *51* (4), 379–382.
(60) De La Calle García, D.; Reichenbächer, M.; Danzer, K.; Hurlbeck, C.; Bartzsch, C.; Feller, K. H. Analysis of wine bouquet components using headspace solid-phase microextraction−capillary gas chromatography. *J. High Resolut. Chromatogr.* **1998**, *21* (7), 373–377.
(61) Ebeler, S. E.; Terrien, M. B.; Butzke, C. E. Analysis of brandy aroma by solid-phase microextraction and liquid-liquid extraction. *J. Sci. Food Agric.* **2000**, *80* (5), 625–630.
(62) Wardencki, W.; Sowiński, P.; Curyło, J. Evaluation of headspace solid-phase microextraction for the analysis of volatile carbonyl compounds in spirits and alcoholic beverages. *J. Chromatogr., A* **2003**, *984* (1), 89–96.
(63) Kataoka, H.; Lord, H. L.; Pawliszyn, J. Applications of solid-phase microextraction in food analysis. *J. Chromatogr., A* **2000**, *880* (1−2), 35–62.
(64) Nose, A.; Hojo, M.; Ueda, T. Effects of salts, acids, and phenols on the hydrogen-bonding structure of water−ethanol mixtures. *J. Phys. Chem. B* **2004**, *108*, 798–804.
(65) Wang, Y.; O'Reilly, J.; Chen, Y.; Pawliszyn, J. Equilibrium in-fibre standardisation technique for solid-phase microextraction. *J. Chromatogr., A* **2005**, *1072* (1), 13–17.
(66) Setkova, L.; Risticevic, S.; Linton, C. M.; Ouyang, G.; Bragg, L. M.; Pawliszyn, J. Solid-phase microextraction-gas chromatography-time-of-flight mass spectrometry utilized for the evaluation of the new-generation super elastic fiber assemblies. *Anal. Chim. Acta* **2007**, *581* (2), 221–231.
(67) Niri, V. H.; Pawliszyn, J. Equilibrium in-fiber standardization method for determination of sample volume by solid phase microextraction. *Analyst* **2007**, *132* (5), 425–430.
(68) Aznar, M.; Tsachaki, M.; Linforth, R. S. T.; Ferreira, V.; Taylor, A. J. Headspace analysis of volatile organic compounds from ethanolic systems by direct APCI-MS. *Int. J. Mass Spectrom.* **2004**, *239* (1), 17–25.
(69) Roberts, D. D.; Elmore, J. S.; Langley, K. R.; Bakker, J. Effects of sucrose, guar gum, and carboxymethylcellulose on the release of volatile flavor compounds under dynamic conditions. *J. Agric. Food Chem.* **1996**, *44*, 1321–1326.
(70) Chirife, J.; Buera, M. P. A simple model for predicting the viscosity of sugar and oligosaccharide solutions. *J. Food Eng.* **1997**, *33* (3−4), 221–226.
(71) Hansson, A.; Andersson, J.; Leufvén, A. The effect of sugars and pectin on flavour release from a soft drink-related model system. *Food Chem.* **2001**, *72* (3), 363–368.
(72) Rabe, S.; Krings, U.; Berger, R. G. Dynamic flavor release from sucrose solutions. *J. Agric. Food Chem.* **2003**, *51*, 5058–5066.
(73) Friel, E. N.; Linforth, R. S. T.; Taylor, A. J. An empirical model to predict the headspace concentration of volatile compounds above solutions containing sucrose. *Food Chem.* **2000**, *71* (3), 309–317.
(74) Czerny, M.; Christlbauer, M.; Fischer, A.; Granvogl, M.; Hammer, M.; Hartl, C.; Hernandez, N. M.; Schieberle, P. Re-investigation on odour thresholds of key food aroma compounds and development of an aroma language based on odour qualities of defined aqueous odorant solutions. *Eur. Food Res. Technol.* **2008**, *228* (2), 265–273.

Received for review July 24, 2009. Revised manuscript received September 30, 2009. Accepted September 30, 2009. This research project was conducted while the primary author (A.L.R.) was an Australian−American Fulbright Scholar and was conducted as a collaboration between The University of California−Davis, Murdoch University, and CSIRO Plant Industry. This research was partially funded by USDA-CSREES-NRI Grant 2005-01244 and Australia's grape growers and winemakers through their investment body, the Grape and Wine Research and Development Corporation, with matching funding from the Australian federal government. The results of this study were presented in part at the American Society for Enology and Viticulture 60th Annual Meeting, June 2009, Napa Valley, CA, and In Vino Analytica Scientia July 2009, Angers, France.